BSc Project
Ecosystem Stability in Rock-Paper-Scissors Games with Different Competition Modes and the Stability Analysis of Equilibrium Points

Guo Jing Yang

31st March 2023

Supervisor: Dr. Dave Clements
Assessor: Dr. Tim Evans

Word Count: 5525 words excluding title page, content page, figure captions, declaration of work done, acknowledgements, appendix and bibliography.

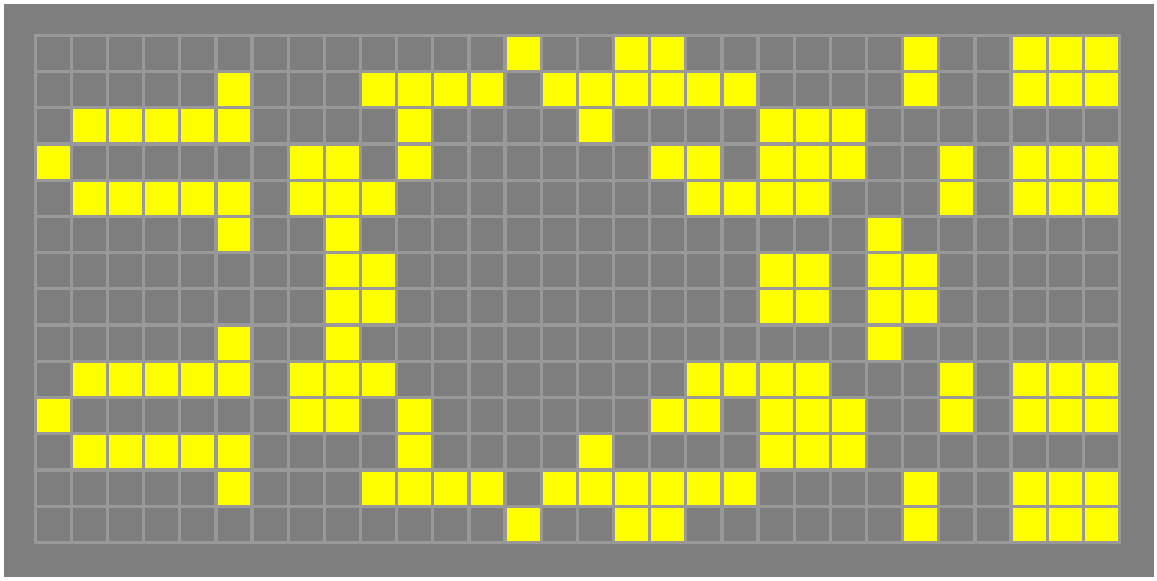

Figure 1: Pattern in Conway's Game of Life. Life Lexicon Identifier: *dragon* (c/6 orthogonally, p6). Categories: *spaceship*[1].

Contents

0 Abstract

Understanding the interaction mechanisms that could lead to a high level of biodiversity in an ecosystem is of imperative importance. Intransitive competition, in which no one species is consistently dominant, plays a crucial role in this problem. In this report, we investigated how different types of interactions and ranges can affect the system stability in a rock-paper-scissors game. We showed that local range interaction and cyclic competition structure led to a stable coexistence ecosystem. For global range interaction, our stochastic model led to monoculture, where only one species survives in the ecosystem. Furthermore, we showed that local selection is more stable against fluctuation in initial abundance, but the movement of individuals can also affect the stability. The difference between deterministic and stochastic models is significant, but it didn't change the qualitative behaviour of the outcome.

We demonstrated that the three-species equilibrium point, ρ^*, is unstable and stochastic effects will cause the system to decay into single species. The contrast to what is seen in the simulation; and is a consequence of the spatial model. The stability of an ecosystem is dependent on the formation of a self-organised structure; each of these structures could oscillate out of phase to preserve community stability. Our study concluded that small changes in the interaction methods could result in stark behaviour changes in the ecosystem, emphasising the importance of accurately identifying the interaction mechanisms and the rarity of biodiversity.

1 Preamble

The coexistence of multiple species in a community has long been studied in ecology. Many mechanisms have been proposed to explain biodiversity. This includes niche differentiation, where each species evolve to occupy different ecological niches within an ecosystem, and neutral theories, where each species in a community are functionally equivalent, with no inherent difference in their ability to survive and reproduce.

Among them, intransitive competition, a type of competition where no one species is consistently dominant over the others, can prevent the emergence of a dominant species and has been supported by empirical evidence across natural communities[2, 3, 4]. It creates a cyclic pattern of species dominance, where each species can outcompete one other species but is outcompeted by another. The classic game of rock-paper-scissors(RPS) provides a model for intransitive competition. Models of communities with this competition structure usually would converge to an equilibrium steady state, given the presence of higher-order interactions. Higher-order interactions are interactions where a pairwise interaction between two species can affect other pairwise interactions[5]. Additionally, population mobility has been discovered to be crucial in regulating ecosystem stability in rock-paper-scissors games. Limited mobility fosters species variety, whereas excessive mobility threatens biodiversity. Embedding communities in space also stabilise their dynamic when interactions are local, but global interactions can produce large oscillations in species abundance and eventually lead to stochastic extinctions.

Additionally, other theoretical studies found that the time evolution of species abundances in a community can be modelled with a set of coupled ordinary differential equations (ODE). Mathematical analysis of this set of equations can provide insight into the stability of the equilibrium points.

Through this project, we aim to investigate how different interaction modes with different spatial scales affect the coexistence of species with intransitive interaction and conduct a mathematical analysis of the stability of equilibrium points.

2 Methods

We consider a system of 3 species with intransitive interaction (e.g. Rock, Paper, Scissors). These species, with a fixed number of individuals N, are arranged in a 2D lattice. One individual can only occupy each site and is independent of the others. This is similar to a spatially explicit cellular automaton model. The competitive-outcome(CO) matrix is as follows:

$$C = \begin{pmatrix} 0 & 0 & 1 \\ 1 & 0 & 0 \\ 0 & 1 & 0 \end{pmatrix} \tag{1}$$

where C_{ij} denotes the probability of species i winning against species j when intransitive competition happens between the two species. If $C_{ij} = 1$, this means that species i outcompetes species j. This follows that species j is outcompeted by i, therefore $C_{ji} = 0$. Thus, the competitive-outcome matrix is "antisymmetrical" about the leading diagonal[6]. Here we set $C_{ii} = 0$, disregarding any intraspecific competition where the same species competes for the same resources. The benefit of using a CO matrix is that we can describe the pairwise interaction between any two species in the community.

To investigate the community dynamics, the simulation is performed as follows:

1. We generate a square lattice with $N = L \times L = 100 \times 100$ individuals, where L is the number of rows/columns of the lattice, with periodic boundary conditions. In periodic boundary conditions, the space is "wrapped around" each spatial axis, i.e. the sites at one end of the lattice are connected to the sites at the opposite end[7, 8].

2. We populate the lattice with individuals where each species has a defined probability of being selected.

3. In each time step, we perform an interaction based on one of the defined processes or a sequence of processes.

4. We repeat step 3 for 2000 time steps, which we had tested to be sufficient for the system to reach a steady state.

5. The number of individuals for each species and the spatial patterns are recorded for each time step.

To investigate the effect of interaction range on ecosystem stability, we look at the two extremes in the interaction range: *local interaction* where the neighbourhood is the Moore Neighbourhood of the focal site and *global interaction* where the neighbourhood consists of all sites in the lattice[9].

2.1 Process 1: Selection

Selection mimics the scenario where species compete for limited resources in the community. In our simulation, the limited resources are the sites (space) in the lattice. In each time step, all individuals will perform one of the selection modes. There are three types of selection/competition modes.

Mode 1 (S1): We look at the focal site's neighbourhood based on its interaction range. We check if the fraction of individuals in the neighbourhood that can outcompete the resident in the focal site is more than a given threshold according to the matrix *C* in Eq. 1: (i) if there are at least 33% superior competitors (relative to the focal resident) surrounding the focal resident, then the focal resident will be replaced by the superior competitors; (ii) if there are less than 33% superior

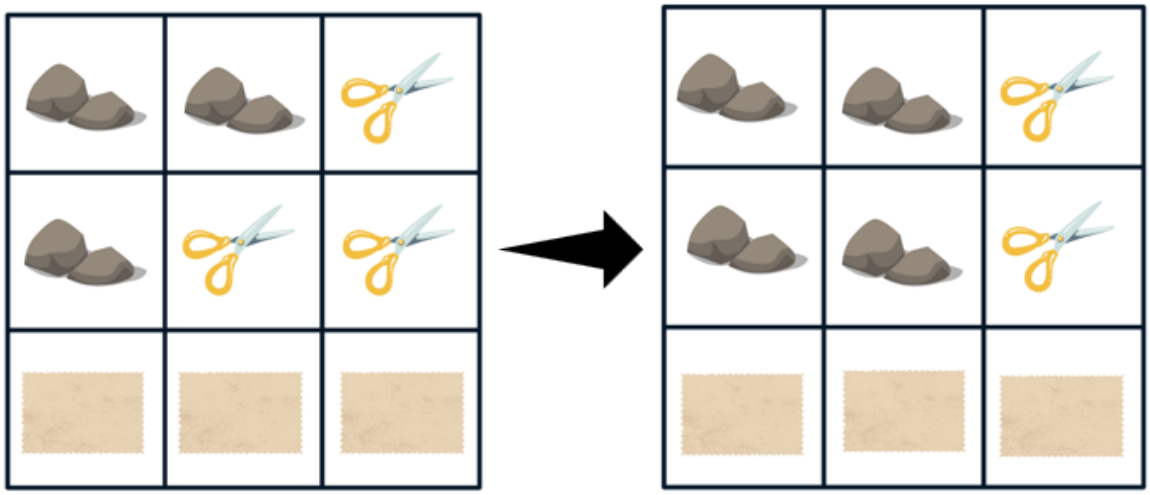

Figure 2: S1 (local): Rock is the superior competitor of Scissor, as there is more than 33% of Rock surrounding Scissor ($\frac{3}{8} \geq \frac{1}{3}$). Scissors is replaced by Rock.

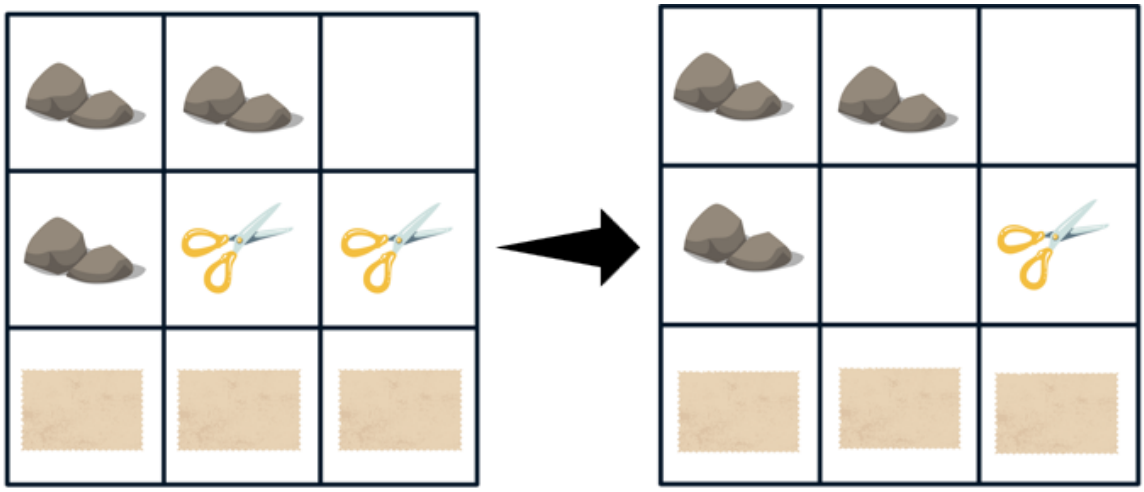

Figure 3: S2 (local): We have the possibility of having an empty site as a neighbour (due to empty sites created from the previous selection). As we don't count empty sites in the denominator, the fraction of the superior competitor, Rock, is now ($\frac{3}{7} \geq 33\%$). An empty site replaces scissors.

competitors, then the resident is unchanged. An example of this is shown in Fig. 2. This mode only works for *local interaction*. For *global interaction*, one species can go extinct if its superior competitor has a species abundance of more than 33% of the total population in any given time step, making the simulation highly unstable.

Mode 2 (S2): This interaction is similar to Mode 1. The only difference is that when there are at least 33% superior competitors surrounding the focal resident, rather than being replaced by the superior competitors, the resident will be withdrawn from the lattice, leaving an empty site. We do not consider neighbouring empty sites in the denominator when counting the fraction of superior competitors, as species don't interact with empty sites. Again, this mode only works for local interaction, but we will define other processes below that modify this to have a global range.

Mode 3 (S3): One neighbour of the focal site is selected randomly. If the selected neighbour outcompetes the focal resident, then the focal resident is replaced by it. Otherwise, nothing

changes. For local interaction, the neighbour is the Moore neighbourhood of the focal site, and for global interaction, it is any individual in the lattice[10].

2.2 Process 2: Reproduction

Reproduction mimics the process where the species increases its abundance in the lattice by reproducing. In each time step, we identify all empty sites in the lattice surrounded by at least one individual in their Moore Neighbourhood. Each identified empty site will be replaced by one of the individuals in its neighbourhood in a stochastic manner. The probability of a species occupying an empty site is proportional to its abundance in the Moore Neighbourhood of the empty site. For example, if an empty site is surrounded by 1 Rock, 3 Papers, 3 Scissors and 1 empty site, then the probability of the focal empty site being replaced by Rock, Paper and Scissors are $\frac{1}{7}$, $\frac{3}{7}$ and $\frac{3}{7}$ respectively. This can be shown in Fig. 4A. We don't count empty sites in the denominator as it cannot reproduce itself. Similarly, if an empty site has all empty sites in its neighbourhood, then it won't reproduce, preserving causality.

2.3 Process 3: Mobility

Mobility provides movement to species in the lattice. In each time step, we identify all the individuals that are unhappy. We denote unhappy individuals as those whose fraction of the same species as the focal individual in their neighbourhood is less than 33%; this is analogue to Schelling Model[11]. With the same reasoning as in S2, we don't count empty sites in the denominator. The threshold of 33% is arbitrary and is chosen to match the threshold in S2. These unhappy individuals will then randomly move to any empty sites in the lattice. An example is shown in Fig. 4B. As the number of empty sites is usually less than the number of unhappy individuals, the unhappy individuals will compete for the empty sites. Since no one species dominate all other species, for simplicity, we randomly select the unhappy individuals to move to the empty sites until all empty sites have been filled. Finally, we replaced the sites that the moved individuals previously occupied with empty sites.

For all of our processes and modes, we have used a discrete-time model or *synchronous updating*; all the sites are updated simultaneously. Therefore, the species' abundance can change drastically in one time step. Another update method is the continuous time model or *asynchronous updating*, in which we randomly select one focal site to perform the changes rather than iterating through all sites in a single time step. A detailed comparison between these two can be found in many research papers; we will here state the general conclusion[12, 13]. For stochastic models, there is little difference between discrete and continuous time models[14, 15]. However, the results are largely different for a deterministic model[16]. In our simulation, only S1 and S2 are deterministic processes; the rest of the processes are stochastic. Still, the reader should not extrapolate that the system is radically different for discrete and continuous time. Most of the basic properties of a cellular automaton model do not depend on the updating method being used[13].

Combining **S2** with **Reproduction** and **Mobility**, we create a new selection mode that has a global range. The exact sequence is [Mobility, Reproduction, S2], and we consider this as one time step. This sequence then repeats itself until it reaches the final time step. In the mobility stage, some individuals move around the lattice. This gives opportunities to the new neighbours of the moved individuals to interact with faraway individuals. The reproduction process is a buffer time step where each species occupies some empty sites. This ensures a sufficient amount of interaction happens in S2 as individuals don't interact with empty sites. As mobility can only happen when there are empty sites available. The first time step of the simulation is set to be S2 to initialise some empty sites. As we will be making comparisons of this new selection mode with S1, we name this mode as **S1 Global**.

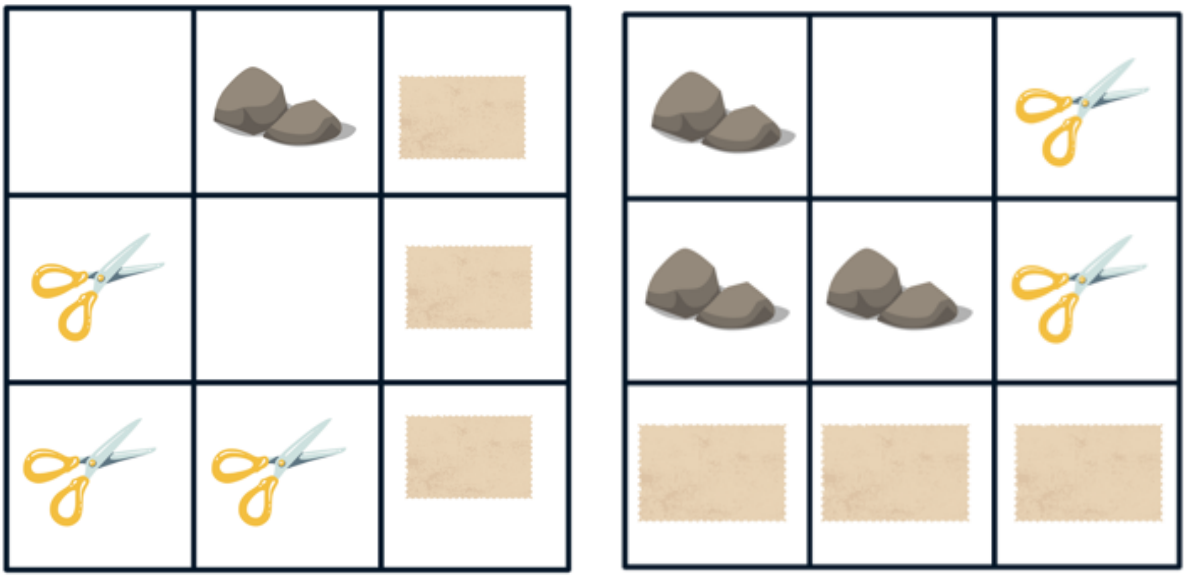

(A) (B)

Figure 4: Fig. 4A shows reproduction process. The probability for the focal empty site to be occupied by R, P and S is $\frac{1}{7}$, $\frac{3}{7}$ and $\frac{3}{7}$ respectively. We don't count empty sites in the denominator as it doesn't reproduce. Fig. 4B shows the mobility process. As the fraction of rock surrounding the focal rock is $\frac{2}{7} \leq 33\%$, the focal rock will move to an empty site in the lattice in the next time step. Again, we don't count empty sites.

3 Numerical Testing

Before carrying out the simulation, we performed unit tests to ensure the code worked as said in the theory.

3.1 Competitive-Outcome Matrix

We checked that for each species, the outcome of the pairwise interaction with other species and itself is according to the matrix *C*.

3.2 Selection Mode 1

With a threshold of 33%, if a focal site is surrounded by more than 3 superior competitors (relative to the focal resident), it will be replaced by the superior competitors. We visualised the simulation and tracked a few sites in the lattice, particularly at the boundaries of interactions. We always observed the simulation agreed with our theoretical prediction.

3.3 Selection Mode 2

The test is similar to S1. However, there may be empty sites surrounding the focal site in S2. Therefore, 3 superior competitors are the upper limit for the focal site to be replaced by an empty site.

3.4 Selection Mode 3

As the interaction in S3 is a stochastic process, we looked for general agreement with our theoretical predictions. We tracked the clusters of the same species in our simulation visualisation. We checked that these clusters were later replaced by their superior competitors. We conducted the test with different initial distributions and time steps, and all of them agreed with the prediction.

3.5 Reproduction

We placed one individual from each species in the lattice, where each individual is equally spaced from the other two individuals, forming an equilateral triangle. We ran the simulation and observed that each species increased in abundance at a similar rate. As the species clashed, we observed that the boundary contained roughly equal amounts of each of the species. When the lattice was fully occupied, the number of individuals for each species was roughly the same, a third of the total number of sites. This agreed with our theoretical prediction as due to the symmetry of the initial setup, the final species abundance should be similar to each other. We did this with multiple realisations to probe the stochastic effects, and the end simulations agreed with the theory every time.

3.6 Mobility

For simplicity in testing, we used a threshold of 50% for mobility. We started with a 10 by 10 square occupied by Rock surrounded by 1 layer of Paper, so in total, it is an 11 by 11 square in a $L = 100$ lattice. All the Papers would be unhappy because the fraction of Rock is more than 50% (we don't count empty sites). The Rocks at the four corners of the square were also unhappy, as 3 Rocks and 5 Papers surrounded them. Therefore, they will stay mobile until the threshold is met. This is what we observed in the simulation. The individuals that stabilised were those that met the threshold; the initial pattern of the Rock square didn't change (except the four corners) throughout the simulation.

4 Results

4.1 Temporal Fluctuation

We begin by examining the temporal population dynamics of the three species, considering both local and global interactions with $L = 100$. Due to the intransitivity of the three species, we expect the species abundance to fluctuate about the equilibrium point, $\rho^* = (\frac{1}{3}, \frac{1}{3}, \frac{1}{3})$ in the steady state[17]. These temporal fluctuations form loops surrounding ρ^* in phase space. These loops arise as a species grows in number by outcompeting another species and subsequently declining due to being outcompeted by the species that it is vulnerable to[2].

Different types of selections and interaction ranges affect the magnitude of temporal fluctuations. With local range selections, the difference in fluctuation sizes between S1 and S3 is small. S1 produces the smallest fluctuation as seen in Fig. 5, and all of them oscillate around ρ^*. For global range selection, the fluctuations are larger than those obtained under local range selections with the same mode as seen in Fig. 6. For S3, the fluctuations are so large that stochastic extinction occurs, leading to a monoculture of Paper. The fluctuations can be better seen via the phase space diagram in Fig. 7.

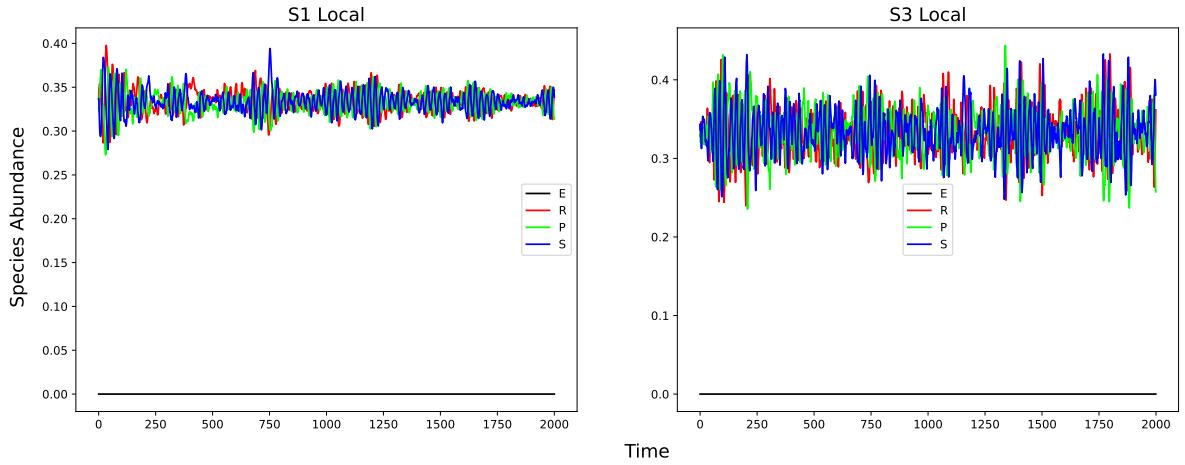

Figure 5: Dynamics of the abundance of a 3 species system in a rock, paper, scissors games with local interactions. The lattice size is $N = L \times L = 100 \times 100$. The abundance is normalised to 1. We observed oscillation with a mean at $\frac{1}{3}$. E in the legend represents empty sites, and RPS represents the three species. The initial species abundance is one-third for all the species.

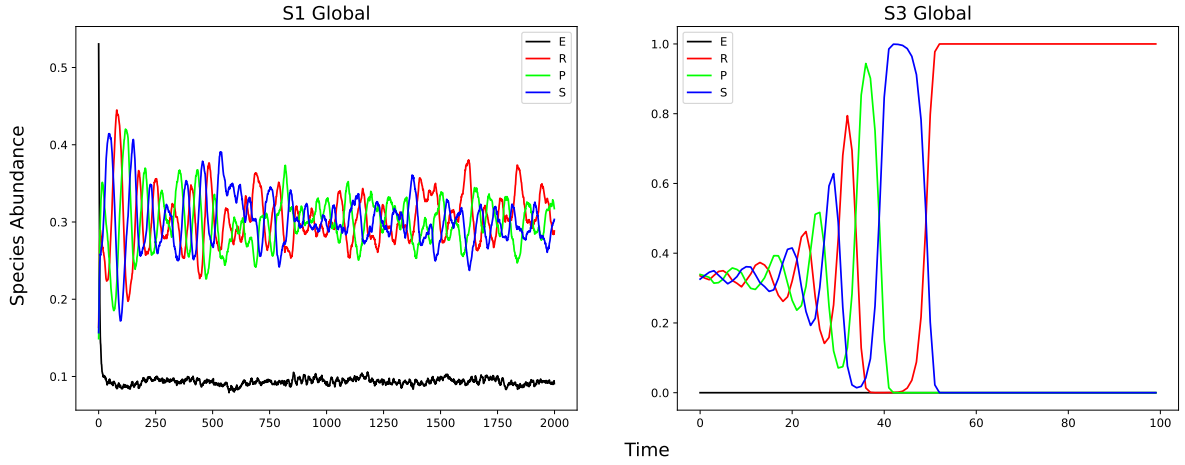

Figure 6: The figures shows the population dynamics as in Fig. 5 but with global interactions. Compared to Fig. 5, the oscillation amplitudes are larger and lead to stochastic extinction for S3.

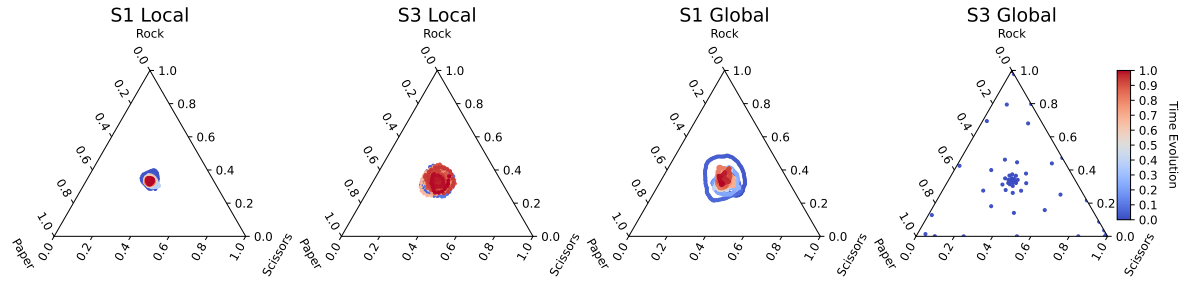

Figure 7: Trajectories in the phase space with different interaction modes and ranges, corresponding to the dynamics in Fig. 5 and 6. The sum of the three species' abundance and the total time step are normalised to 1. Large oscillation amplitude around the ρ^* corresponds to broader area coverage, indicating a more unstable system. The temporal evolution of S3 Global is an outward spiral shape, which can be seen by connecting the dots.

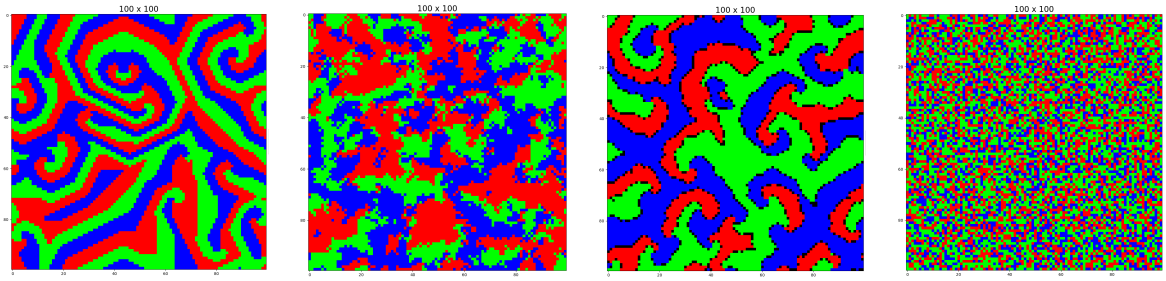

(S1 Local) (S3 Local) (S1 Global) (S3 Global)

Figure 8: Snapshot of the spatial organisation of the ecosystem in the steady state (except for S3 Global, where the steady state is a monoculture) with lattice size $L \times L = 10^4$ for different selection modes and interaction ranges. Snapshot for S3 Global was taken at a few time steps before it entered stochastic extinction. The colour RGB corresponds to Rock, Paper and Scissors.

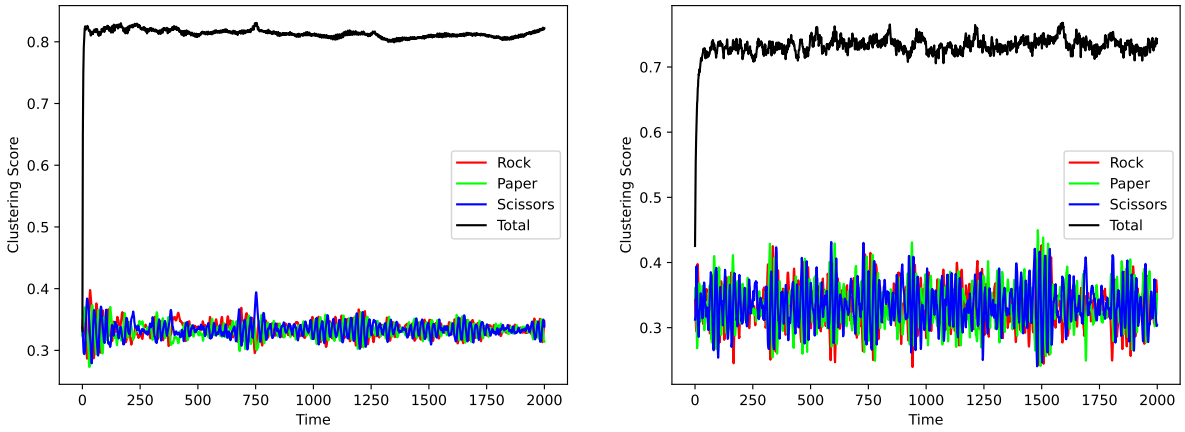

(S1 Local) (S3 Local)

Figure 9: Clustering score for different selection modes with local interaction and initial species abundance of one-third.

4.2 Spatial Organisation

Various selection methods and scopes also have an impact on the community's spatial organisation. In the case of local interaction, species gather into spatial clusters, excluding other species from these specific areas, forming conspecific clusters. Whereas for global interaction, it depends on the selection modes. S1 Global formed large clusters, while for S3 Global, no spatial organisation emerged. To measure the degree of clustering, we devised an algorithm that calculates how similar each individual is to its Moore Neighbourhood; if it is similar to all of them, it will get a score of 1, and 0 if it is not similar to any of them[8]. We then take the average score for each species and also the average score of all species.

From Fig. 9 and 10, we can see the clustering score for each selection mode and range. For local selection, S1 has a higher clustering score. This is because S3 is a stochastic process where the composition of the local area can change drastically compared to S1 (especially at the boundary); this can be seen in Fig. 8. The fluctuation seen in the S3 clustering score in Fig. 9 also indicates the rapid change in local composition. The generally high clustering score for local selection is due to the emergence of self-organised spatial structures.

S1 Global has the highest clustering score among all the selection modes considered. This

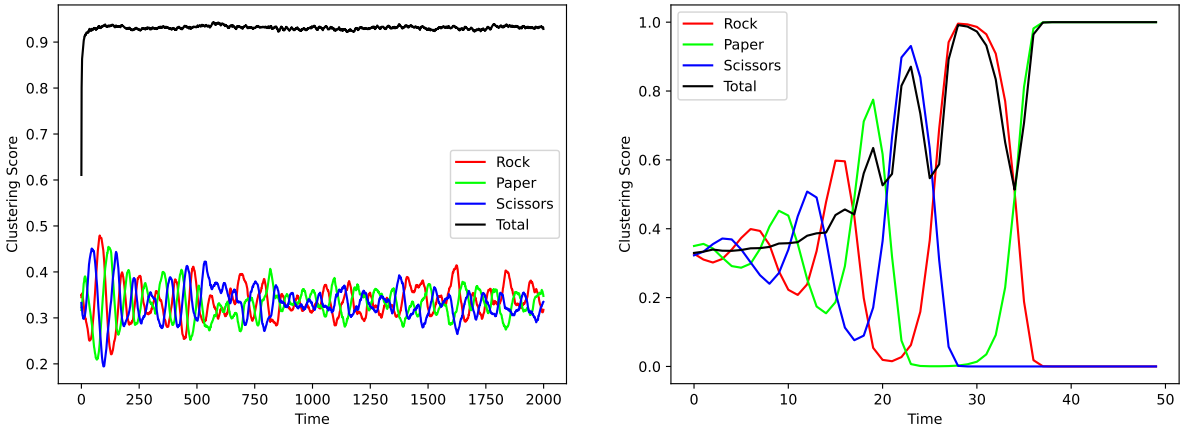

(S1 Global) (S3 Global)

Figure 10: Clustering score for different selection modes with global interaction and initial species abundance of one-third. The clustering scores for Total and Paper reach 1 due to stochastic extinction in S3 Global

is due to the combined effect of selection and mobility. In S1 Global, the mobility process moves almost all individuals not in a cluster, as they will be unhappy, to the empty sites left out by S2 (usually at the boundary of clusters). This will then undergo S2 after the reproduction stage. In short, this moves individuals not in a cluster to the boundary of clusters to undergo selection. The result will be a high clustering score. For S3 Global, the ecosystem ends in monoculture, so the clustering score is 1. The high clustering score here does not indicate biodiversity but the elimination of other species.

We observe a correlation between the fluctuation in clustering score to the temporal fluctuation in species abundance. This can be seen by relating the area coverage in Fig. 7 to the oscillation amplitude in Fig. 9 and Fig. 10. Generally, stochastic models have greater fluctuations. Some alert readers may notice the difference in fluctuation for S1 Global. This is due to the transient state in S1 Global having a large fluctuation which obscures the small fluctuation in the steady state in Fig. 7.

4.3 Local Interaction with Different Neighbourhood

We also looked at the effect of the neighbourhood on local interaction. The two other types of neighbourhoods we looked at were von Neumann and extended von Neumann neighbourhoods[18]. The class of von Neumann neighbourhood represents the set of sites that is orthogonally adjacent to the focal site. An example of both neighbourhoods is shown in Fig. 11. The von Neumann neighbourhood contains one site in each orthogonal direction, whereas the extended von Neumann contains two[19]. The reason to include neighbours two sites away in the extended von Neumann is such that the total neighbours are the same as the Moore Neighbourhood.

Fig. 12 shows the spatial organisation of the ecosystem with initial abundance equal to ρ^*. The interaction mode is S1 Local but with different neighbourhoods. The ecosystem stopped changing after reaching a steady state, and all species are able to coexist. The reason is that in the von Neumann neighbourhoods, all sites are restricted to only interact in the orthogonal direction. This reduces the number of configurations available for the system, which in turn greatly reduce the number of configurations where the focal site is replaced by its stronger competitor, the probability of this happening is approximately 41% (see Appendix for the derivation). Similar arguments apply to Extended von Neumann; the probability is even smaller, as it has more neighbours. As there are more configurations in the Moore Neighbourhood, we will focus our

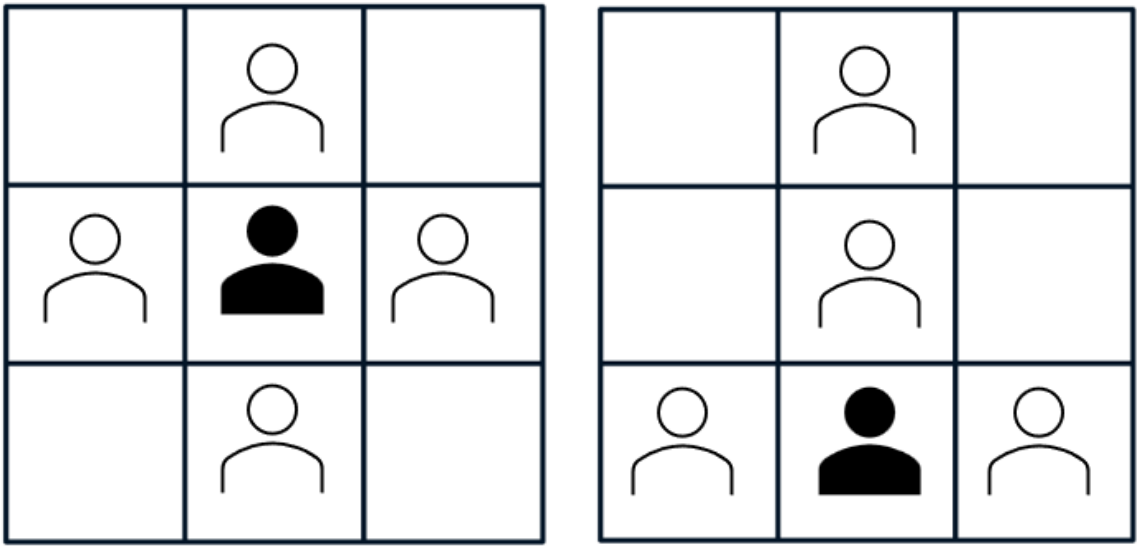

(von Neumann) (Extended von Neumann)

Figure 11: The four orthogonally adjacent sites are the neighbourhood for von Neumann. There are two sites in each orthogonal direction of the focal site for extended von Neumann, making a total of 8 neighbours; the figure only shows the top site completely.

analysis on it for the rest of the report.

4.4 Community stability with initial species abundance

We now extend our exploration of different interaction modes and ranges to various initial species abundances. We generated 2278 different initial points that are equally spaced in the phase space diagram, ρ^* was one of the points. For each initial point, we initialised the lattice with 100 different realisations and performed the simulation on each of them. After the final time step, we compared the spatial patterns of the last two frames. If they aren't the same, the system is in an oscillation state. If they are the same, the system is either in a non-oscillating stable coexistence state or, more commonly, stochastic extinction. We found that the number of times it is in a stable coexistence state is less than 1% among all the simulations with the same last two frames, and it only happens for deterministic models. The reason that this happened is that some focal sites are surrounded by their stronger competitor with a number lower than the threshold required to change the focal sites. This is just an artefact due to the threshold, and these simulations will lead to monoculture if the threshold isn't present. Therefore we can ignore this and refer to the number of times the simulation has the same last two frames as the Extinction Frequency.

Fig. 13 shows a contour plot of the phase space diagram for local range selection. Interaction via S3 is very stable, leading to coexistence at ρ^* in the long run for most initial species abundance. In the extreme cases where the initial abundance of one of the species is close to 1, extinction happens as there are mainly pairwise interactions in the community, and the effect of higher-order interaction is negligible. Interaction via S1 is less stable. If the difference between species abundance is larger than 0.2 (roughly), stochastic extinction can happen. The reason S3 is more stable than S1 against changes in initial abundances is due to the type of interaction. The focal site only interacts with one neighbouring site in S3 Local compared to the eight neighbouring sites in S1 Local. This leads to a slower interaction rate and hence gradual changes in species abundance in the transient state. As seen in Sec.4.1, large fluctuation in abundance causes stochastic extinction. Therefore, S1 is more susceptible to stochastic extinction. How-

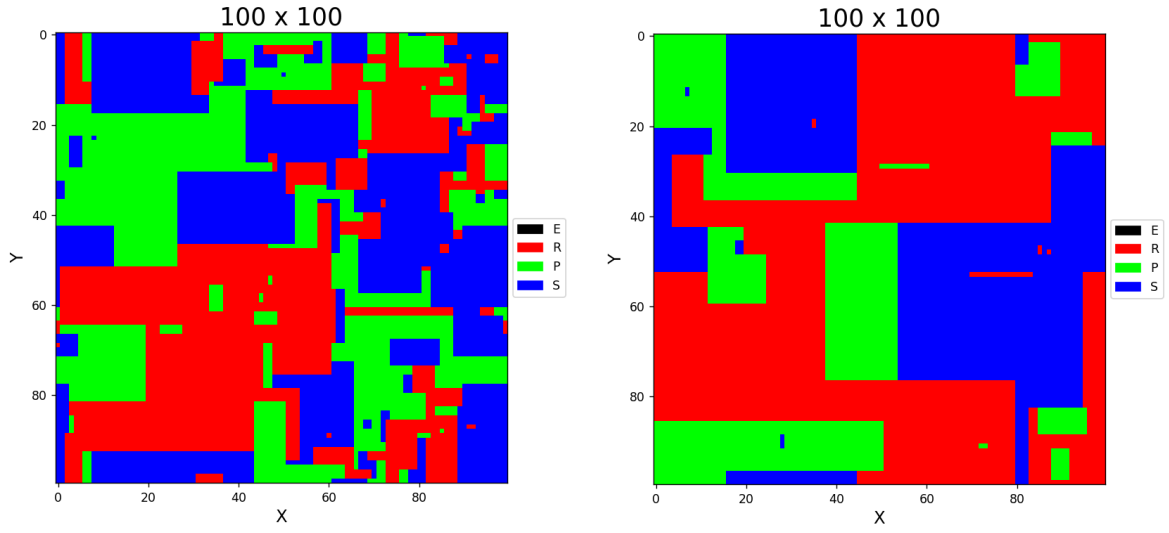

(von Neumann) (Extended von Neumann)

Figure 12: Snapshot of the spatial organisation of the ecosystem in steady state ($t = 150$) with initial species abundance equal to ρ^*. Biodiversity emerges in both cases, with larger conspecific clusters for Extended von Neumann.

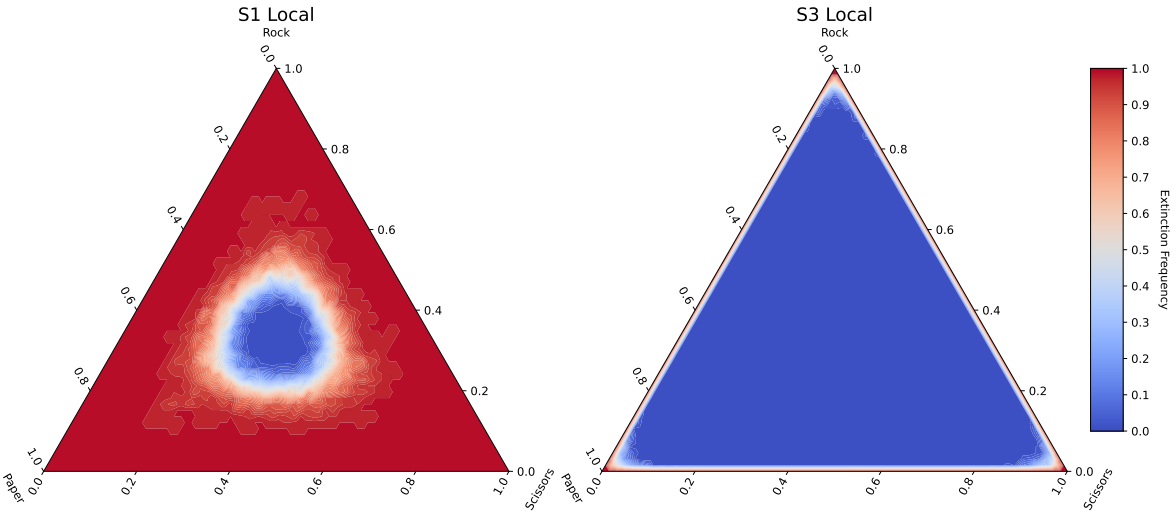

Figure 13: Contour phase space diagram for local range selection with a total of 2278 unique points. The colour density of each point represents the normalised extinction occurrence, with the dark red colour (1.0) representing extinction happening in every realisation.

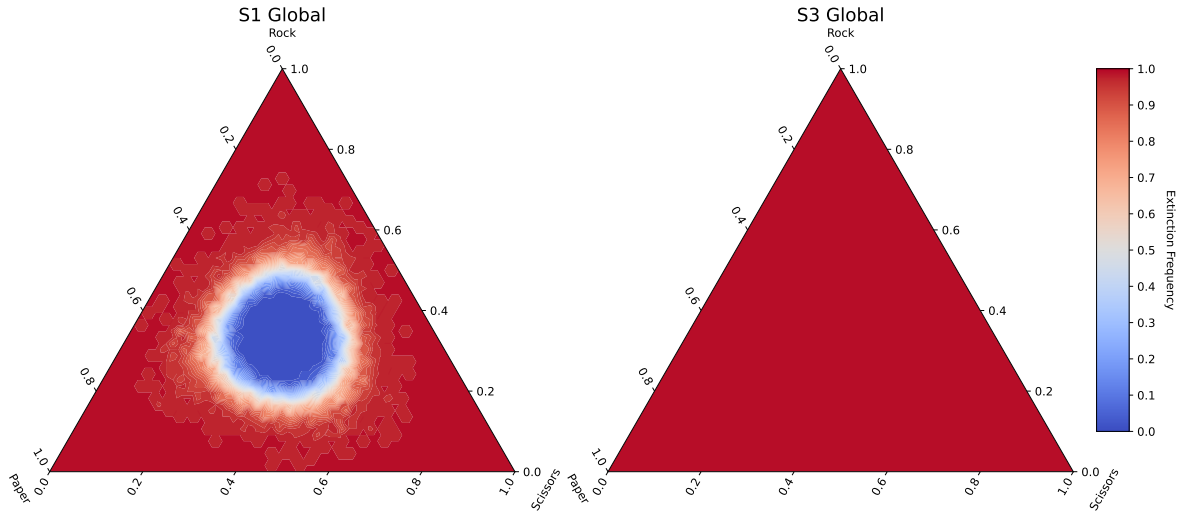

Figure 14: Contour phase space diagram for global range selection with a total of 2278 unique points. S3 Global leads to monoculture for any initial species abundance, indicating this type of interaction is highly unstable. However, S1 Global has more stable initial points compared to S1 Local.

ever, you may have noticed from Fig. 5,7,9,10 that S3 has larger temporal fluctuations. These fluctuations are due to the stochastic evolution of S3 compared to the deterministic evolution in S1. They are much smaller in amplitude than the transient' oscillations we discussed here.

Fig. 14 shows a contour plot of the phase space diagram for global range selection. We see that global interactions are more sensitive to the change in initial abundance, with none leading to biodiversity in S3 Global. This is not surprising as the presence of local selection can lead to the development of self-organised spatial structure within a habitat, which is impossible under global selection. Specifically, under short-range competition, clusters of single species tend to expand as the species with the highest local density has a larger probability of occupying nearby sites.

Additionally, the composition of the local area is not altered due to the absence of intraspecific competition, leading to the development of large conspecific clusters. Consequently, the overall community dynamics slow down since selection interactions, which cause changes in species abundance, occur only at the cluster boundaries, and these boundaries only represent a small fraction of the entire habitat. With global interaction, all sites are equidistant, and the results of the selection have a strong correlation with the total abundance of each species rather than local abundance. This implies that when one species gains a population advantage, it continues to increase its abundance by outcompeting its weaker rival. This, in turn, alleviates the competition pressure on its stronger competitor, enabling it to grow in abundance by outcompeting the former species. This leads to a global succession cycle and large oscillation amplitudes of abundance in the transient state. When the fluctuations exceed the threshold of the total number of individuals, other species will go extinct, leading to monoculture[2].

Based on our previous arguments, we would expect S1 Global also lead to monoculture. However, S1 Global is not a mere extension of the neighbourhood range as in S3 Global but a combination of different processes. The mobility process in S1 global preserves intransitivity-mediated coexistence from the local selection as only the unhappy individuals will move[20]. This resists the breakdown of conspecific clusters formed by species aggregation and inhibits the mixing of individuals in the lattice. However, the sites that the unhappy individuals moved to are empty sites left out by the previous selection. This results in greater mixing of individuals at the boundaries of clusters which prevents stable coexistence. The effect of the latter is only significant in the transient state, as there were many unhappy individuals due to the random initial

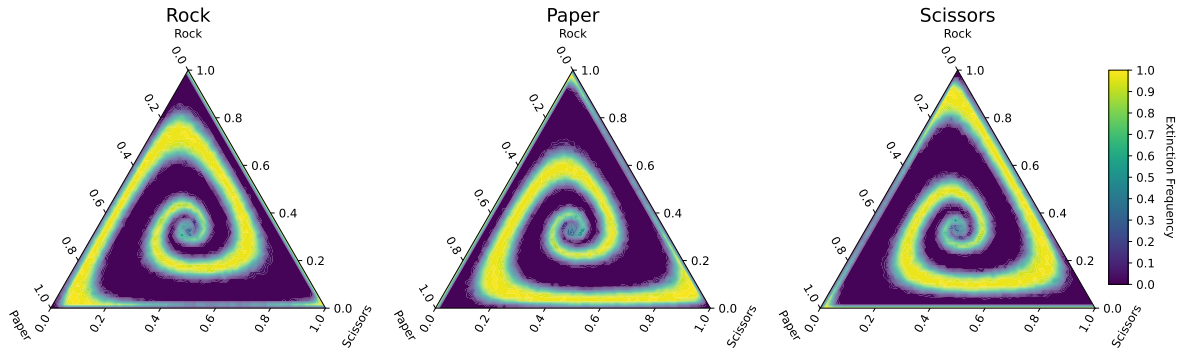

Figure 15: From left to right, each subplot shows the normalised number of times the system ends up in the monoculture state of rock, paper, and scissors, respectively, for each initial point under S3 Global. A yellower point means a higher number of monocultures. There is a rotation symmetry due to intransitivity. The summation of the three subplots equals the right subplot in Fig. 14.

distributions. Therefore, if there isn't a stark contrast in the initial abundance, which can lead to monoculture due to mobility, the ecosystem will enter a coexistence state. These two mechanisms compete with each other, which eventually leads to a similar, if not larger, coexistence area in the phase space diagram compared to S1 Local.

For S3 Global in Fig. 14, we plotted the number of times it led to a monoculture of Rock, Papers and Scissors over 100 realisations in Fig. 15. With initial points near ρ^*, the number of times it ends with monoculture is roughly the same for each species. There is a rotation symmetry in the phase space diagram, which is expected due to intransitivity. In Fig. 16, we plotted the initial species abundance distribution, which leads to a monoculture of **Paper** in a 3D plot; only the initial distributions that have a 100% success rate were plotted. These points can be categorised into two main categories.

The first category is a straight line in the Rock-Paper axis where the abundance of Scissors is negligible. This corresponds to the thin yellow line connecting Rock-Paper in the Paper's diagram in Fig. 15. As there is only pairwise interaction between Rock and Paper, Paper will dominate the lattice (competitive exclusion principle).

The second category is the spiral shape; this corresponds to the spiral shape we see in Fig. 15. We see that when the initial Rock abundance is low (roughly ≤ 0.2) in Fig. 15, it will lead to a monoculture of Paper. This is because there are mainly Paper-Scissors competitions at the beginning, which alleviate competition pressure on Rock. This allows it to grow rapidly in abundance, which then gives an advantage to Paper which is now low in abundance. This may happen in multiple succession cycles until reaching a monoculture of Paper. This corresponds to the thick yellow line at the base of the Paper's triangle in Fig. 15. However, if the initial Scissors abundance is too low (roughly ≤ 0.15), then the majority of Paper will shield Scissors from the competition. The same succession cycle happens until reaching the monoculture of Rock. This corresponds to the thick yellow line parallel to the left side of the Rock's triangle. This tells us a small initial abundance of a species' stronger competitor doesn't always benefit that species.

4.5 Analysis on the stable equilibrium point solutions

From Fig. 13 and Fig. 14, we see that different initial species abundance will result in oscillation or extinction solutions. For initial points near ρ^*, they will oscillate around ρ^* due to intransitive competition. For points that lead to monoculture, the solutions are the 3 single population points: (1, 0, 0), (0, 1, 0), (0, 0, 1), each corresponding to the survival of one species. For initial points

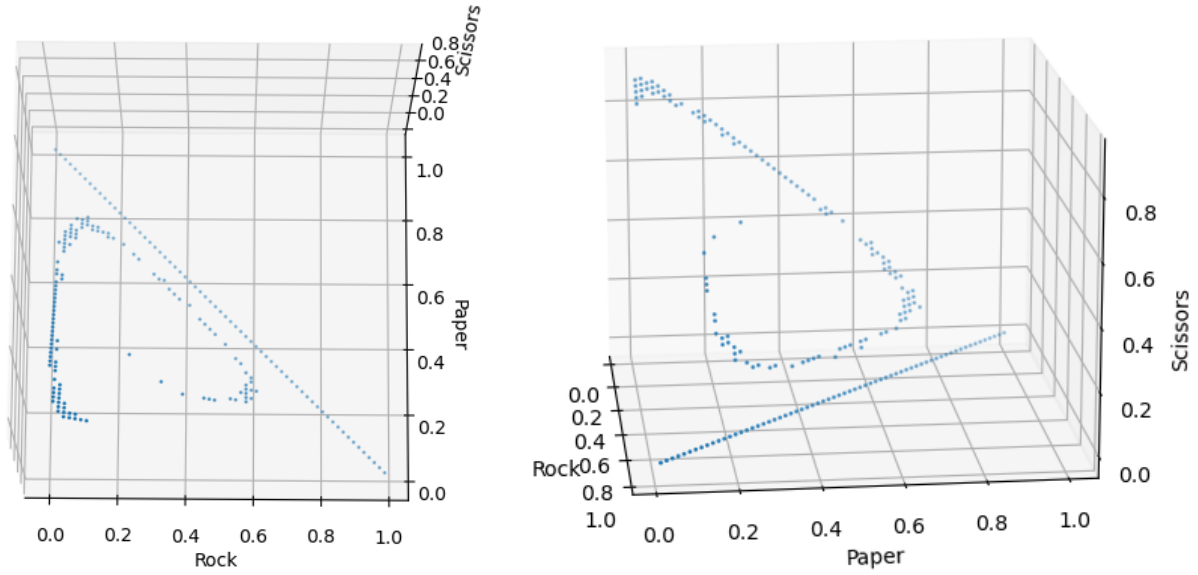

(Paper: Top) (Paper: Front)

Figure 16: This is a 3D scatter plot of the initial points, which results in the monoculture state of Paper. Each axis represents the species abundance of that species. There are two categories: (i) a straight line in the Rock-Paper axis and (ii) a spiral shape.

at the transition boundary, the final solutions can be either of the two categories. We can model these dynamics with a mean field ODE, also known as the Lotka-Volterra(LV) competition model. We named the three species 1, 2, and 3, and they have competitive relations as stated in the CO matrix ($1 < 2 < 3 < 1$). The species abundance of each species can be described using the following equations:

$$\begin{aligned} \frac{dn_1}{dt} &= n_1(\beta_{13}n_3 - \beta_{21}n_2) \\ \frac{dn_2}{dt} &= n_2(\beta_{21}n_1 - \beta_{32}n_3) \\ \frac{dn_3}{dt} &= n_3(\beta_{32}n_2 - \beta_{13}n_1) \end{aligned} \tag{2}$$

where n_i is the normalised abundance of species i, and β_{ij} is a constant which relates the probability of species i invades species j, its value can be read from the CO matrix. Therefore, $\beta_{13}n_3$ represents the rate at which species 1 invades species 3 and $\beta_{21}n_2$ represents the rate at which species 1 get invaded by species 2. These are the only two terms as we disregard intraspecific competition. The rates are then multiplied by n_1 to obtain the ODE of the abundance of species 1. A similar form is seen for the ODE of the other two species due to the cyclic symmetry of the interaction. All the β_{ij} in Eq. 2 have values of 1 from the CO matrix. The solutions of the ODE equations are a family of periodic orbits surrounding the equilibrium point, ρ^* (see Appendix for proof). The analysis is similar to that of May and Leonard (1975), who considered the symmetric system[21].

$$\begin{aligned} \frac{dN_1}{dt} &= N_1\{1 - N_1 - \alpha N_2 - \beta N_3\} \\ \frac{dN_2}{dt} &= N_2\{1 - \beta N_1 - N_2 - \alpha N_3\} \\ \frac{dN_3}{dt} &= N_3\{1 - \alpha N_1 - \beta N_2 - N_3\} \end{aligned} \tag{3}$$

where N_i is the scaled number of individuals in species i such that the competition coefficient of intraspecific competition, λ_{ii} is 1. The competition coefficient, λ_{ij}, is a measure of the extent to which species j affects the growth of species i. α represents the competition coefficient between a species and its stronger competitor, and β represents the competition coefficient between a species and its weaker competitor. β here is different to the β_{ij} in Eq. 2. From Eq. 3, the competition coefficient matrix, λ is

$$\lambda = \begin{pmatrix} 1 & \alpha & \beta \\ \beta & 1 & \alpha \\ \alpha & \beta & 1 \end{pmatrix} \tag{4}$$

If we introduce $N = N_1 + N_2 + N_3$, we can rewrite this equation as

$$\begin{aligned} \frac{dN_1}{dt} &= N_1(1-N) - (\alpha-1)N_1N_2 - (\beta-1)N_1N_3, \\ \frac{dN_2}{dt} &= N_2(1-N) - (\alpha-1)N_2N_3 - (\beta-1)N_2N_1, \\ \frac{dN_3}{dt} &= N_3(1-N) - (\alpha-1)N_3N_1 - (\beta-1)N_3N_2. \end{aligned} \tag{5}$$

Let $\gamma = \alpha + \beta - 2$, we add the equations to get

$$\frac{dN}{dt} = N(1-N) - \gamma\left\{N_1N_2 + N_2N_3 + N_3N_1\right\} \tag{6}$$

When $\alpha + \beta = 2$, $\gamma = 0$. This implies that the plane $N_1 + N_2 + N_3 = 1$ is invariant. In Eq. 2 we have $n_1 + n_2 + n_3 = 1$ as they were normalised, therefore substituting $N = 1$ into Eq. 5, and by comparison to Eq. 2, $\alpha = 2,\ \beta = 0$. The reason $\beta = 0$ is due to the different assumptions of the intrinsic growth rate of a species, r. In Eq. 3, it is assumed that r is larger than 0, whereas, for our simulation, it is 0 without combining reproduction. Nonetheless, the qualitative behaviour of their solutions is the same[13]. The three-species equilibrium point, ρ^*, is stable if and only if all eigenvalues of λ have positive real parts[21]. The eigenvalues of λ can be written down as

$$\begin{aligned} \lambda_1 &= 1 + \alpha + \beta \\ \lambda_{2,3} &= 1 - (\alpha+\beta)/2 \pm i(\sqrt{3}/2)(\alpha-\beta) \end{aligned} \tag{7}$$

Substituting $\alpha = 2,\ \beta = 0$, we have $\lambda_1 = 3,\ \lambda_{2,3} = \pm i\sqrt{3}$. Therefore, ρ^* is not a stable equilibrium point. The system is only neutrally stable on the plane $N_1 + N_2 + N_3 = 1$.

The LV competition model derived above is based on continuous time. To implement the model into our system, we discretised Eq. 2 and the equation becomes as follows:

$$n_i(t+1) - n_i(t) = \sum_j n_i(t)\left\{\beta_{ij} - \beta_{ji}\right\} n_j(t) \tag{8}$$

where t represents the t^{th} time step. As mentioned in Sec. 2, the discretisation of time would not alter the basic properties of the system. To solve the discrete coupled ODE in Eq. 8, we used a second-order predictor-corrector method[22]. We used the explicit Euler method as the predictor to predict the values of $n_i(t+1)$ and the implicit second-order Adams-Moulton (AM2) method to correct $n_i(t+1)$ to the final value. The whole procedure can be shown below:

$$\begin{aligned} f_a &= f\left(t_m, n_m^i, n_m^{j,k}\right) \\ f_b &= f\left(t_{m+1}, n_m^i + f_a\Delta t, n_m^{j,k} + f_a\Delta t\right) \\ n_{m+1}^i &= n_m^i + \frac{1}{2}\left(f_a + f_b\right)\Delta t \end{aligned} \tag{9}$$

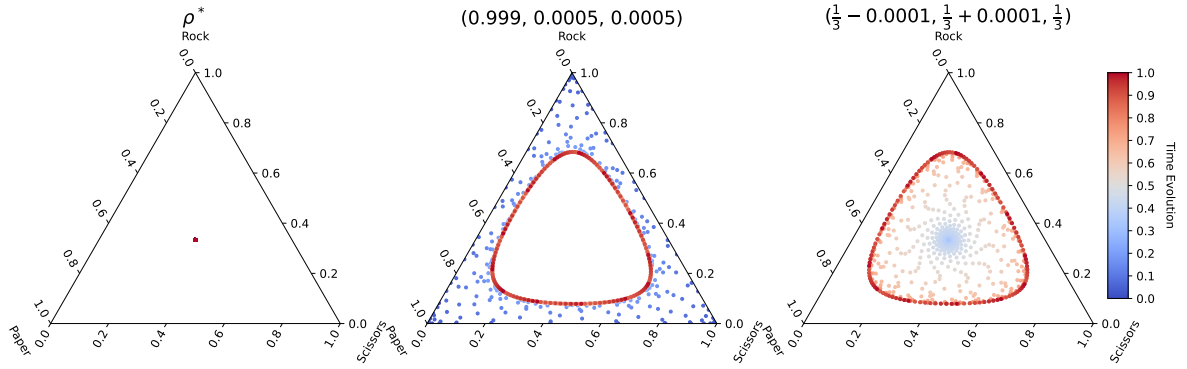

Figure 17: Temporal evolution of the system with different initial points in the phase space diagram. The initial points are shown in the plot title. The total time step for all three plots is 1000 and is normalised. We see that ρ^* is stable against time evolution. However, the other two extreme initial points converge to the red loop with time. The trajectory of these plots are spirals that go inward for the middle plot and outwards for the right plot. The reason for this slightly confusing plot is that the plotting software doesn't allow density line plots.

where t_m is the m^{th} time step from the initial time, n_m^i is the abundance of species i at time t_m and $f\left(t_m, n_m^i, n_m^{j,k}\right)$ is a function representing the first derivative of the abundance of species i at time t_m; this is dependent on other species.

Fig. 17 shows the time evolution of species abundance in the phase space diagram using the predictor-corrector method. The initial points for the three diagrams are shown in the plot title. We see that if the initial point is ρ^*, the species abundance will stabilise on the equilibrium point. However, with a slight shift in the initial point, as shown on the right plot, it spirals outwards. From theory, the solution for each initial point is a periodic orbit characterised by its distance from ρ^* in the phase space and has the form of $H(n) = \sum_i \rho_i \log n_i$, where x_i is the i^{th} index of point ρ^* and n_i is the normalise species abundance. The deviation seen in Fig. 17, where different initial points converge to the same periodic orbit, is unusual. Based on a rough investigation, this could be due to the scaling issues. As we increment $\Delta t = 1$ in the AM2 method, the changes in n_m^i are typical of the scale of 10^{-3}; the difference in scale might lead to the abundance of each species being overly or underly dependent on the previous species abundance of other species (i.e. β_{ij} might be larger or smaller than 1). This results in the solution moving to an orbit where the changes in n^i are comparable to $\Delta t = 1$ such that it is now not overly or underly dependent on the previous species and stabilises on the periodic orbit. Most initial points will converge to the red loop, with examples shown in Fig. 17. Nevertheless, this still demonstrates that ρ^* is not a stable equilibrium point.

Comparing the results in Fig. 17 to Fig. 7, we saw in the long time limit, the system either stabilizes with a loop smaller than in Fig. 17 (S1 Local, S3 Local and S1 Global) or lead to monoculture as in S3 Global. This is different from the theory. Stochastic effects from the neighbour selection in S3 will cause the system to move between the family of solutions and eventually decay to a single species system[13, 23]. This is seen in our simulation for S3 Global in Fig. 6,7. However, this solution does not apply to the stochastic spatial model (S3 Local). For local range selection, the self-organised structures will have their species' abundance oscillate out of phase with respect to each other. This results in a stable equilibrium density for each of the three types. The same explanation can be applied to the deterministic spatial model (S1). This agrees with our results as shown in Fig. 6,7. The Lotka-Volterra competition model can't be applied to S1 Global as it doesn't take into account mobility nor reproduction[13].

5 Conclusion

Our analysis verifies that merely having cyclic dominance is insufficient to preserve biodiversity. Specifically, S3 Global leads to a monoculture in the long term despite a cyclic competition structure. Furthermore, we deduce that local interactions are more conducive to fostering biodiversity than global interactions[2]. Schelling's Mobility can increase the stability of the system, provided the initial difference in abundance isn't that significant. The deterministic model (S1) and stochastic model (S3) have different tolerance to temporal fluctuations and initial points. S3 Local has a larger tolerance against monoculture in initial points, whereas the temporal fluctuations in S1 Local are smaller. Therefore, the interaction rule must be defined accurately before modelling the community.

In conclusion, we successfully showed that biodiversity depends on interaction rules and ranges. Stochastic effects can cause the system to deviate from the unstable equilibrium point, ρ^* and lead to the extinction of species. This project can be taken further by looking at (i) interaction ranges between the two extremes; (ii) different interaction rules; (iii) the effect of larger system sizes on interaction ranges and rules; (iv) the difference between *synchronous* and *asynchronous* updating method; (v) competition between more species; (vi) competition between species with different dominance degree (i.e. a Rock can win Scissors with a given probability rather than 1).

6 Declaration of Work Undertaken

Apart from the last stage of the project, the work was done together. We would split the coding task and papers to read evenly. For coding, we would break down the coding tasks into smaller chunks, and each of us takes half of it. We will review code changes from each other before merging into the main branch on GitHub. For theory, we would each summarize important points in the papers we read that can be implemented. Regular discussions were held to discuss any issues, ideas and goals. In the last stage, I mainly worked on the mathematical analysis of equilibrium points (LV competition model) while my project partner investigated how different processes and sequences affect the community stability on initial points (less discussed in this report). We decided to do so due to time constraints and our interest in looking at both directions.

7 Acknowledgements

Firstly, I would like to thank the Physics Department for having this project. I have learnt many things, especially how to conduct research independently. Secondly, I would like to thank Dr Dave Clements for supervising this project. During our meetings, he provided us with questions to ponder upon and pushed us to analyse our findings critically. He helped us a lot in shaping our goals and objectives for this project. Lastly, I would also like to extend my gratitude to my project partner. His enthusiasm and commitment to this project motivated me to work diligently on this project. He also constantly provided a new perspective on things that I overlooked. Without his skills and hard work, we would not achieve so many things in these 3 months.

8 Appendix

8.1 Probability Calculation

In Sec. 4.3, we mentioned that the probability that a focal site will get replaced by its stronger competitor is 41% in the von Neumann neighbourhood. Here is a detailed breakdown of the calculation. We assumed that the system started with all species having roughly equal numbers. Therefore, for each site, it will have an equal probability of being either of the species. To find the probability, we list down all possible cases where the focal site is replaced. Here we use [T, L, R, B] to represent the species occupying the top, left, right, and bottom of the focal site. For example, [R, R, R, R] means Rock occupies all the sites. Due to the cyclic symmetry, it doesn't rely on which species occupy the focal site. We will take the case that the focal site is Rock.

Case 1: A focal site is fully surrounded by its stronger competitor.
Total number = 1
Configurations: [P, P, P, P]

Case 2: A focal site is surrounded by 3 stronger competitors.
Total number = 4 $\times$ 2 = 8
4 came from the different orientations of the sequence; it is then multiplied by 2 because the remaining could be either of the other 2 species.
Configurations:[P, P, P, R], [P, P, P, S], [P, P, R, P], ...

Case 3: A focal site is surrounded by 2 stronger competitors.
Total number = 6 $\times$ 4 = 24
6 came from the different orientations of the sequence; it is then multiplied by 4 to account for the different orientations of the remaining species.
Configurations: [P, P, R, R], [P, P, R, S], [P, P, S, R], [P, P, S, S], [P, R, P, R], [P, R, P, S], ...

The total number of cases is $3^4 = 81$. Therefore, the total probability is

$$P(replaced) = \frac{33}{81} = 41\% \tag{10}$$

In our simulation, the sites are related. However, compared to Moore Neighbourhood, the correlation is weaker in the von Neumann and extended von Neumann neighbourhoods. Therefore, in the long time limit, all sites will reach species equilibrium as each site has a higher tendency of not changing.

8.2 Periodic orbit solution

In Sec. 4.5, we claimed that the solution to Eq.2 is a periodic orbit surrounding ρ^* in phase space. For convenience, I will restate the differential equations here.

$$\begin{aligned}
\frac{dn_1}{dt} &= n_1(\beta_{13}n_3 - \beta_{21}n_2) \\
\frac{dn_2}{dt} &= n_2(\beta_{21}n_1 - \beta_{32}n_3) \\
\frac{dn_3}{dt} &= n_3(\beta_{32}n_2 - \beta_{13}n_1)
\end{aligned} \tag{11}$$

We define the steady point as $\vec{\rho}$ = (ρ_1, ρ_2, ρ_3). At $\vec{\rho}$, $\frac{dn_i}{dt} = 0$. Dividing each equation by the product of betas in it, we obtain

$$\frac{\rho_3}{\beta_{21}} = \frac{\rho_2}{\beta_{13}} = \frac{\rho_1}{\beta_{32}} \tag{12}$$

We drop the second subscript in β_{ij} for brevity. Multiplying by $\beta_1\beta_2\beta_3$, we obtain

$$\begin{aligned}\rho_1 &= \frac{\beta_3}{\beta_1+\beta_2+\beta_3}\\ \rho_2 &= \frac{\beta_1}{\beta_1+\beta_2+\beta_3}\\ \rho_3 &= \frac{\beta_2}{\beta_1+\beta_2+\beta_3}.\end{aligned} \tag{13}$$

To find that there is a family of periodic orbit solutions surrounding $\vec{x}$, we can write $H(n) = \sum_i \rho_i \log n_i$ and note that

$$\begin{aligned}\frac{\partial H}{\partial t} &= \sum_i \frac{\rho_i}{n_i}\frac{d\rho_i}{dt}\\ &= c\left(\frac{\rho_3}{\beta_2}-\frac{\rho_2}{\beta_1}\right)+c\left(\frac{\rho_1}{\beta_3}-\frac{\rho_3}{\beta_2}\right)+c\left(\frac{\rho_2}{\beta_1}-\frac{\rho_1}{\beta_3}\right)=0,\end{aligned} \tag{14}$$

where $c = \frac{\beta_1\beta_2\beta_3}{\beta_1+\beta_2+\beta_3}$. Thus, the Hamiltonian, H, is constant along the solutions of the ODE. In the phase space diagram, $H(n)$ has a solution of orbits with ρ^* as the centre.

8.3 Different interaction sequences

In the report, we only looked at the community stability with initial abundance for [Mobility (M), Reproduction (R), S2]. Here we will look at two other combinations, which are [S2, R, M] and [S2, R, S2, R, M]. We will drop the 2 for brevity. We will use the same setup as the S1 Global in Fig. 14 except that the sequence is different now. Due to the large amount of computational resources required, we only have 50 realisations for each initial point.

Fig. 18 shows the contour phase diagram for different sequences. SMR and SRSRM have roughly the same stability radius, whereas SRM has a smaller stability radius. The difference can be explained by mobility. As seen from S1 Local in Fig. 13 and S1 Global in Fig. 14, having mobility increases the stability radius. However, in SRM, after selection, the reproduction phase will replenish the empty sites. The stronger competitors near the empty sites have a higher chance of occupying the empty sites simply because they eliminated the weaker competitors in the previous phase. Therefore, in the mobility phase after that, the weaker competitors will move away, as there are even more stronger competitors surrounding them now. In SMR, the mobility phase happens right after selection. As selection leaves empty sites between the boundaries and individuals do not interact with empty sites, fewer individuals are being moved compared to SRM. Similar to SRSRM, fewer individuals are being moved because mobility happens less frequently. We see here that an adequate amount of mobility is crucial to maintaining biodiversity.

8.4 50% Mobility

We also investigated the effect of increasing mobility by changing the threshold. Previously, the focal site would only move if the fraction of the same species in the neighbourhood dropped below 33%. Here, we increased it to 50%, with everything else the same as in Fig. 18. In Fig. 19, we see the same trend as in Fig. 18, but the stability radius is smaller than their counterpart in Fig. 18, this is due to the same reason that there are too many individuals being moved.

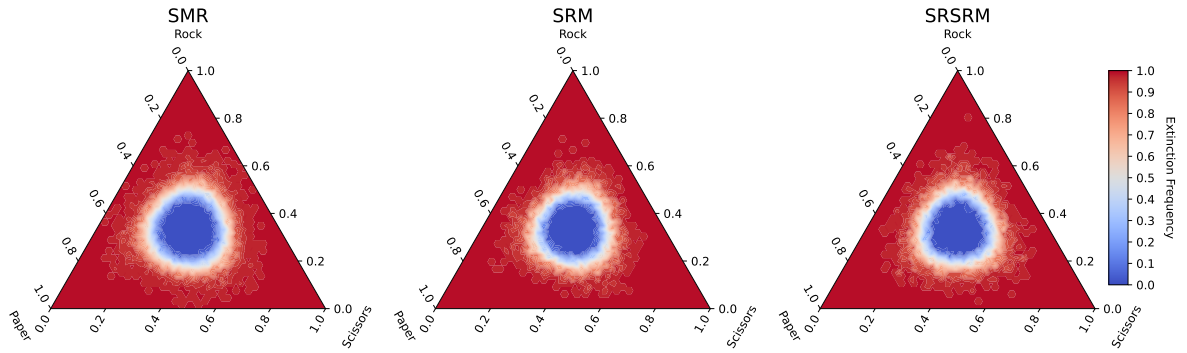

Figure 18: Contour phase space diagram for SMR, SRM and SRSRM, the initial setup is the same as S1 Global in Fig. 14 except for the sequencing of the process. SRM has the smallest stability radius, while SMR and SRSRM have roughly the same stability radius.

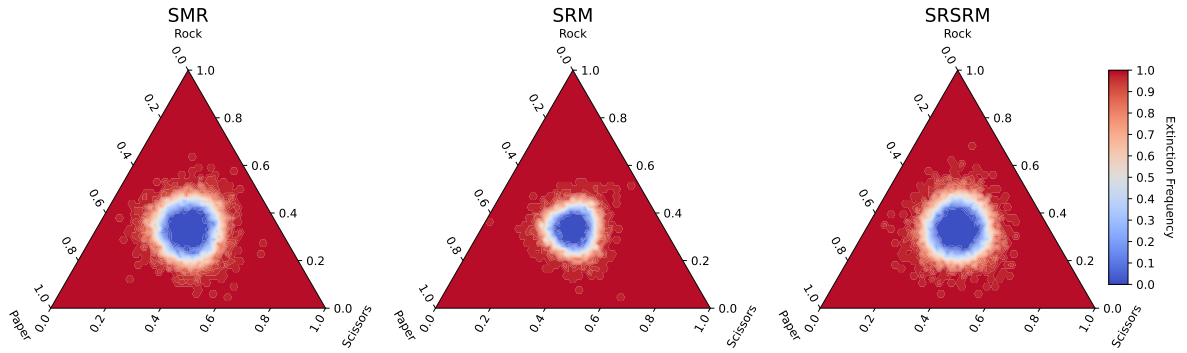

Figure 19: Contour phase space diagram for SMR, SRM, SRSRM with a similar setup as in Fig. 18, the only difference is the threshold for mobility is 50%. The stability radius is smaller than its counterpart in Fig. 18.

References

[1] S. A. Silver, “Life lexicon,” 2023, last accessed 12 April 2023. [Online]. Available: https://bitstorm.org/gameoflife/lexicon/#nl6

[2] Z. Zhang, D. Bearup, G. Guo, H. Zhang, and J. Liao, “Competition modes determine ecosystem stability in rock–paper–scissors games,” *Physica A: Statistical Mechanics and its Applications*, vol. 607, p. 128176, 2022.

[3] S. Allesina and J. M. Levine, “A competitive network theory of species diversity,” *Proceedings of the National Academy of Sciences*, vol. 108, no. 14, pp. 5638–5642, 2011.

[4] J. M. Levine, J. Bascompte, P. B. Adler, and S. Allesina, “Beyond pairwise mechanisms of species coexistence in complex communities,” *Nature*, vol. 546, no. 7656, pp. 56–64, 2017.

[5] J. Grilli, G. Barabás, M. J. Michalska-Smith, and S. Allesina, “Higher-order interactions stabilize dynamics in competitive network models,” *Nature*, vol. 548, no. 7666, pp. 210–213, 2017.

[6] R. A. Laird and B. S. Schamp, “Competitive intransitivity promotes species coexistence,” *The American Naturalist*, vol. 168, no. 2, pp. 182–193, 2006.

[7] Wikipedia, “Cellular automaton,” 2022, last accessed 2 April 2023. [Online]. Available: https://en.wikipedia.org/wiki/Cellular_automaton

[8] A. Downey, *Think complexity: complexity science and computational modeling*. ” O’Reilly Media, Inc.”, 2018.

[9] Wikipedia, “Moore neighbourhood,” 2022, last accessed 2 April 2023. [Online]. Available: https://en.wikipedia.org/wiki/Moore_neighborhood

[10] M. Frean and E. R. Abraham, “Rock–scissors–paper and the survival of the weakest,” *Proceedings of the Royal Society of London. Series B: Biological Sciences*, vol. 268, no. 1474, pp. 1323–1327, 2001.

[11] E. Hatna and I. Benenson, “The schelling model of ethnic residential dynamics: Beyond the integrated-segregated dichotomy of patterns,” *Journal of Artificial Societies and Social Simulation*, vol. 15, no. 1, p. 6, 2012.

[12] D. Griffeath, “Cyclic random competition: A case history in experimental mathematics,” *AMS Notices*, vol. 35, pp. 1472–1480, 1988.

[13] R. Durrett and S. Levin, “Spatial aspects of interspecific competition,” *Theoretical population biology*, vol. 53, no. 1, pp. 30–43, 1998.

[14] M. A. Nowak and R. M. May, “The spatial dilemmas of evolution,” *International Journal of bifurcation and chaos*, vol. 3, no. 01, pp. 35–78, 1993.

[15] M. A. Nowak, S. Bonhoeffer, and R. M. May, “More spatial games,” *International Journal of Bifurcation and Chaos*, vol. 4, no. 01, pp. 33–56, 1994.

[16] B. A. Huberman and N. S. Glance, “Evolutionary games and computer simulations.” *Proceedings of the National Academy of Sciences*, vol. 90, no. 16, pp. 7716–7718, 1993.

[17] Wikipedia, “Intransitivity,” 2022, last accessed 4 April 2023. [Online]. Available: https://en.wikipedia.org/wiki/Intransitivity

[18] P. Avelino, B. de Oliveira, and R. Trintin, “Lotka-volterra versus may-leonard formulations of the spatial stochastic rock-paper-scissors model: The missing link,” *Physical Review E*, vol. 105, no. 2, p. 024309, 2022.

[19] Wikipedia, “Von neumann neighborhood,” 2020, last accessed 3 May 2023. [Online]. Available: https://en.wikipedia.org/wiki/Von_Neumann_neighborhood

[20] R. A. Laird and B. S. Schamp, “Does local competition increase the coexistence of species in intransitive networks,” *Ecology*, vol. 89, no. 1, pp. 237–247, 2008.

[21] R. M. May and W. J. Leonard, “Nonlinear aspects of competition between three species,” *SIAM journal on applied mathematics*, vol. 29, no. 2, pp. 243–253, 1975.

[22] Wolfram, “Predictor-corrector methods,” 2023, last accessed 10 April 2023. [Online]. Available: https://mathworld.wolfram.com/Predictor-CorrectorMethods.html

[23] M. E. Gilpin, “Limit cycles in competition communities,” *The American Naturalist*, vol. 109, no. 965, pp. 51–60, 1975.